Biomethane is produced by acetate cleavage, not direct interspecies electron transfer: genome-centric view and carbon isotope

Jian Liu, Jiafeng Yu, Yang Tan, Run Dang, Meng Zhou, Marcela Hernández, Eric Lichtfouse, Leilei Xiao

Bioresource Technology 387 (2023) 129589

https://doi.org/10.1016/j.biortech.2023.129589

Biomethane is produced by acetate cleavage, not direct interspecies electron transfer: genome-centric view and carbon isotope

Jian Liu [a,1], Jiafeng Yu [a,1], Yang Tan [b], Run Dang [b], Meng Zhou [c], Marcela Hernández [d], Eric Lichtfouse [e], Leilei Xiao [b,*]

[a] Shandong Key Laboratory of Biophysics, Institute of Biophysics, Dezhou University, Dezhou 253023, PR China
[b] CAS Key Laboratory of Coastal Environmental Processes and Ecological Remediation, Yantai Institute of Coastal Zone Research, Chinese Academy of Sciences, Yantai 264003, PR China
[c] State Key Laboratory of Black Soils Conservation and Utilization, Northeast Institute of Geography and Agroecology, Chinese Academy of Sciences, Harbin 150081, PR China
[d] School of Biological Sciences, University of East Anglia, Norwich NR4 7TJ, UK
[e] State Key Laboratory of Multiphase Flow in Power Engineering, International Research Center for Renewable Energy, Xi'an Jiaotong University, Xi'an, Shaanxi 710049, PR China

HIGHLIGHTS

- Kinetic analysis showed antibiotic exposure stimulated methanogenesis.
- Metagenome-assembled genomes (MAGs) discovered functional microbiomes.
- Network analysis revealed targeted cooperation responding to antibiotic exposure.
- Isotope tracing confirmed the dominance of acetoclastic methanogenesis.

GRAPHICAL ABSTRACT

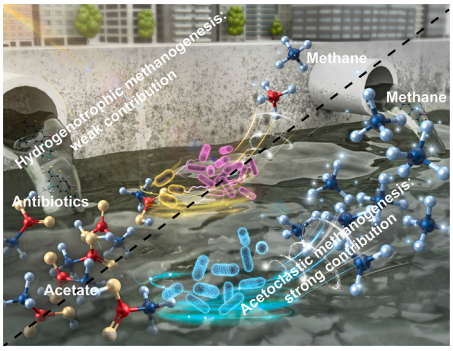

ARTICLE INFO

Keywords:
Metagenome-assembled genome
Acetate metabolism
Antibiotic exposure
Anaerobic digestion

ABSTRACT

Understanding the source of methane (CH_4) is of great significance for improving the anaerobic fermentation efficiency in bioengineering, and for mitigating the emission potential of natural ecosystems. Microbes involved in the process named direct interspecies electron transfer coupling with CO_2 reduction, i.e., electrons released from electroactive bacteria to reduce CO_2 into CH_4, have attracted considerable attention for wastewater treatment in the past decade. However, how the synergistic effect of microbiota contributes to this anaerobic carbon metabolism accompanied by CH_4 production still remains poorly understood, especial for wastewater with antibiotic exposure. Results show that enhancing lower-abundant acetoclastic methanogens and acetogenic bacteria, rather than electroactive bacteria, contributed to CH_4 production, based on a metagenome-assembled genomes network analysis. Natural and artificial isotope tracing of CH_4 further confirmed that CH_4 mainly

* Corresponding author at: Yantai Institute of Coastal Zone Research, 17 Chunhui Road, Laishan District, Yantai, Shandong 264003, China.
E-mail address: llxiao@yic.ac.cn (L. Xiao).
[1] These authors contribute equally.

originated from acetoclastic methanogenesis. These findings reveal the contribution of direct acetate cleavage (acetoclastic methanogenesis) and provide insightsfor further regulation of methanogenic strategies.

1. Introduction

Atmospheric methane (CH_4) is a powerful greenhouse gas, which plays a major role in controlling the Earth's climate. Depending on the approach used, total CH_4 emissions from natural and anthropogenic sources range between 538 and 884 Tg yr^{-1} (Saunois et al., 2020), accounting for 16–25% of atmospheric warming to date (Etminan et al., 2016; IPCC, 2014). Specially, the latest comprehensive assessment from the International Energy Agency reported global CH_4 emissions of about 580 M metric tons in 2021, of which about 60 % comes from human activities (IEA, 2021). A better understanding of the anthropogenic contribution to global CH_4 emissions is therefore critical for a more robust understanding of atmospheric CH_4 change. On the other hand, optimizing biomethane production is also needed to develop sustainable fuels and waste/wastewater treatment (Cavalcante et al., 2021; Xiao et al., 2021a). Despite this importance, microbial CH_4 production mechanisms in man-made environments remain poorly understood compared to natural ecosystems (De Bernardini et al., 2022; Hultman et al., 2015).

Currently, mechanisms explaining CH_4 production include acetoclastic methanogenesis, hydrogenotrophic methanogenesis, and direct interspecies electron transfer (DIET)–CO_2 reduction. Acetate is the classical intermediate in the organic biomass degradation to produce biomethane by acetoclastic methanogens in anaerobic niches (Eq. 1) (Conrad, 2005; Xiao et al., 2020b). Acetoclastic methanogenesis has been estimated to account for two-thirds of the one billion metric tons of CH_4 produced annually in Earth's biosphere (Conrad, 2005; Prakash et al., 2019), despite only a few methanogens, *Methanosarcina* and *Methanosaeta*, are known to transform acetate into CH_4 (Holmes and Smith, 2016). *Methanosarcina* and *Methanosaeta* also have the potential to reduce CO_2 to CH_4 (Dong et al., 2022), and dominate in the artificial anaerobic system (Eq. 2) (Dong et al., 2022; Wang and Lee, 2021).

Acetoclastic methanogenesis: $CH_3COO^- + H^+ \rightarrow CH_4 + CO_2$(1)

Hydrogenotrophic methanogenesis: $4H_2 + CO_2 \rightarrow CH_4 + 2H_2O$(2)

DIET-CO_2 reduction: $8H^+ + 8\ e^- + CO_2 \rightarrow CH_4 + 2H_2O$(3)

DIET involves the direct transfer of electrons from electroactive bacteria to methanogenic archaea, which reduces CO_2 into CH_4 (Eq. 3) with higher efficiency compared to mediated interspecies electron transfer (MIET) by the diffusion of H_2/formate (Stams and Plugge, 2009). DIET-CO_2 reduction is thought to be an important process in anaerobic systems, especially in wastewater, because it does not rely on the exchange of diffusible molecules (Jin et al., 2022; Kumar et al., 2021). Nevertheless, *Geobacter* is the only bacteria with evidence to establish syntrophism with methanogens via DIET (Rotaru et al., 2013; Van Steendam et al., 2019). Therefore, CH_4 generation by DIET-CO_2 is attributed to indirect evidence, and these experimental observations require validation (Van Steendam et al., 2019; Wang and Lee, 2021).

Antibiotics, widely used in human medical practice and livestock husbandry, show a substantial increase in wastewater, threatening the environment and human health (Langbehn et al., 2021; Zhang et al., 2021). Antibiotic residuals alter the composition of microorganisms in wastewater and affect the performance of anaerobic digestion (Yang et al., 2021; Zhi et al., 2019). The influence of different antibiotics on biogas production, however, is unpredictable. Some studies showed a stimulating effect on CH_4 production with the highest increase of 59.97% (Tang et al., 2022; Wang et al., 2022; Zhi and Zhang, 2019). In contrast, an inhibition effect of up to 40% was also reported (Mitchell et al., 2013; Zeng et al., 2021). Antibiotics inhibit the syntrophic or competitive bacteria of methanogenic archaea, which seems to fluctuate CH_4 production in wastewater (Xiao et al., 2021b; Zhi et al., 2019; Zhi and Zhang, 2019). Yet the persistent knowledge gaps about the intrinsic methanogenic strategies have always limited the anaerobic wastewater treatment process and efficiency (Hua et al., 2022; Langbehn et al., 2021; Xiao et al., 2021b).

In this study, metagenome-assembled genomes (MAGs) analysis identified some functional units, such as electricigens and electron-accepting methanogens, but co-occurrence networks analysis suggested a marginal contribution from DIET-CO_2 reduction. Two hypotheses were proposed: (1) microbiota more than individual microbe actively respond to antibiotic exposure; (2) acetoclastic methanogenesis outcompetes DIET to control wastewater methanation.

2. Materials and methods

2.1. Microcosm experiments

The artificial wastewater for the subsequent experiments was referred to the previous study (Song et al., 2019). For all microcosm experiments, three cycles of vacuum/charging high-purity N_2 were conducted to create the anaerobic environments. Norfloxacin or ciprofloxacin was added as the antibiotics-bearing wastewater. The concentration of the antibiotics was monitored by fixed-point sampling throughout the experimental process. Acetate was used as the substrate for bacteria and methanogen with a final concentration of ~30 mM. Vials were incubated at room temperature (25 °C) and mesophilic temperature (35 °C). Samples were sacrificed in triplicate to test the concentrations of acetate, CH_4, H_2, and CO_2 after 24 days of incubation (Xiao et al., 2020b, 2020a).

2.2. DNA extraction, separation, and sequencing

About 0.5 g of sludge was collected on day 8 for metagenomic DNA sequencing, when the antibiotic had a significant effect on the CH_4 concentrations ($P < 0.01$). The total DNA was extracted using E.Z.N.A.® Soil DNA Kit (Omega Bio-tek, Norcross, GA, U.S.) according to the manufacturer's instructions. The extracted total DNA was eluted in nuclease-free water, sheared, and sent for paired-end library preparation with fragment insert sizes of approximately 400 nt. Paired-end (PE) libraries were constructed using NEXTflex™ Rapid DNA-Seq Kit (Bio Scientific, Austin, TX, USA). Adapters containing the full complement of sequencing primer hybridization sites were ligated to the blunt end of fragments. The library was sequenced by using Illumina Hiseq Xten (Illumina Inc., San Diego, CA, USA) at Wefindbio Technology Co., Ltd. (Wuhan, China). Because one sample did not get enough sequencing data, only two of the triplicates in the control group were kept for the downstream analysis. Sequence data associated with this project have been deposited in the NCBI Short Read Archive database (Accession Number: PRJNA734822).

2.3. Assembly of metagenomic data sets

The de novo assembly of metagenomic sequences was conducted on a Linux server with 88 CPU cores and 1 TB RAM. Trimmomatic was applied to remove adapters and filter low-quality reads. The resulting reads were aligned to the human genome Hg38 by BBmap (https://sourceforge.net/projects/bbmap/) to remove contaminations. The final clean reads of all eight samples were co-assembled using MEGAHIT with default parameters. The final contigs were filtered, and only contigs > 500 bp were selected for downstream analysis. The quality of the

assembly was assessed by QUAST.

2.4. Genomic binning and annotation

The binning process was performed with MetaWRAP. Briefly, the assembly was binned with MaxBin2, MetaBAT2, and CONCOCT using the binning module, respectively. The produced bins were refined using the bin_refinment module with completeness > 50, and contamination < 10 as the thresholds. The filtered bins were further improved through the bin_reassembly module, which reassembled the bins by SPAdes. The final bins were quantified through the bin_quant module, which first quantified the contigs by Salmon and calculated the average counts of the whole bins, then normalized each bin as copies per million reads.

The taxonomy annotation of the bins was performed with GTDB-Tk. It first predicted the ORFs of the bins by Prodigal, then 120 single-copy proteins of bacteria and 122 single-copy proteins of archaea were retrieved and aligned with the GTDB database. The concatenated alignment was used to build a phylogenetic tree. Meanwhile, the average nucleotide identity (ANI) of the bins was calculated by FastANI. The taxonomy annotation was performed based on their position on the phylogenetic tree and the ANI similarity.

The ORFs of the bins were predicted by Prodigal, with the default parameters. The final protein sequence files were annotated with eggNOG-Mapper, which aligns the protein sequences to their pre-build database and annotates their function, KEGG assignment, GO assignment, and COG assignment by the best hit.

2.5. Phylogenetic analysis

The genomes were subjected to GTDB-Tk to align the single-copy proteins. Then the concatenated alignments were used to build the phylogenetic tree using IQtree with 100 times bootstrap. Known syntrophic acetate-oxidizing bacteria (SAOBs) were obtained from experiments validated studies (Yu et al., 2022).

2.6. Composition analysis

Kraken2 was applied to assess the microbial composition at the reads level. With Kraken2, the reads were aligned with the RefSeq database, and the taxonomy assignments were selected through the LZW ancestor algorithm. The alpha diversity was calculated at species levels with the Microbiome package (https://microbiome.github.com/microbiome) in R (https://www.r-project.org). The Bray-Curtis distance and PCoA analysis were calculated based on species count with the Vegan package in R.

2.7. Potential c-type cytochrome prediction

Proteins were considered c-type cytochromes if their sequence contained at least one CXXCH motif for covalent heme-binding (where X can be anything except one of [CFHPW]). The motif screening on the protein sequences was performed with ScanProsite.

2.8. Co-occurrence network analysis

The co-occurrence networks of the MAGs in each group were constructed using the CoNet application in Cytoscape with duplicated abundance data. The Pearson, Spearman, Bray-Curtis, and Kullback-Leibler correlation methods were chosen to evaluate pairwise associations among the MAGs, with the initial threshold of 1000 positive and 1000 negative edges from each method. The compositionality bias was alleviated by 1000 renormalized permutations and 1000 bootstrap scores. Edges with Benjamini-Hochberg adjusted p value<0.01 were kept for the co-occurrence networks, which were visualized with the igraph package in R.

2.9. Isotopic analysis and inhibition of acetoclastic methanogenesis

Carbon stable isotope fractionation and artificial abundance isotope tracing with 3% or 6% $^{13}CH_3COONa$ (Merck KGaA, Darmstadt, Germany) as substrates were conducted. Gases collected from the headspace were used to test the δ^{13}C-values of CH_4 and CO_2. CH_3F was applied to inhibit the progress of acetoclastic methanogenesis. Some amount of nitrogen was replaced with 1.5% CH_3F gas as previously reported (Xiao et al., 2020a,b).

2.10. Statistical analysis

Data were presented as mean ± standard deviation of triplicate cultures. All statistical analyses were performed with SPSS 19.0 (SPSS Inc., Chicago, USA) and Origin 8.5 (Origin Lab Corporation, USA) software. A one-way analysis of variance with HSD's test was used to analyze the significance level, and a p-value < 0.05 was considered statistically significant.

3. Results and discussion

3.1. CH_4 production with antibiotic exposure

Anaerobic treatment of eutrophic wastewater is one of the few proven, economical, and friendly strategies. Due to the production of abundant CH_4 during this progress, partitioning of methanogenic strategy would be of great interest to allow better management (Guo et al., 2021; Mancini et al., 2021). Unlike the negative effects of antibiotics on bacteria, these substances created a more favorable environment for biogenic CH_4 production (Figure 1a), especially from the influence of ciprofloxacin. Consequently, the maximum CH_4 yield significantly increased (p = 0.015 for ciprofloxacin, p = 0.023 for norfloxacin).

3.2. Microbiome composition

To unveil the impact of antibiotics on microbial community, the microbial diversity was analyzed based on high-quality reads. The Shannon and Inverse Simpon Index, which reflex the complexity and evenness of the community (Hultman et al., 2015), demonstrated that antibiotics decreased microbial diversity (p = 0.0012 for ciprofloxacin, p = 0.0023 for norfloxacin, Figure 1b). The principal coordinates analysis (PCoA) on the Bray-Curtis distances, which can show the dissimilarity among samples (De Bernardini et al., 2022), further confirmed this tendency with noticeable community differences (p = 0.032, Figure 1c). On the phylum level, both norfloxacin and ciprofloxacin decreased the proportion of *Proteobacteria* (p = 0.033 for ciprofloxacin, p = 0.041 for norfloxacin) while increased *Euryarchaeota* (p = 0.041 for ciprofloxacin, p = 0.045 for norfloxacin) (Figure 1d). The favorable CH_4 production performance could have resulted from the increased abundance of methanogens belonging to *Euryarchaeota*.

Metagenomic binning technology was reported to isolate genomes of individual species (MAGs) from the mixed sequencing data based on sequence characteristics such as abundance, GC percentage, etc. (Chen et al., 2020). Similarly, MAG analysis was applied to further explore the microbiome variation at the species level in this study. Over 100Gbp of high-quality metagenome sequencing data were co-assembled, resulting in 284,942 contigs with an N50 of 9,179 bp (see supplementary material). 246 unique bacterial and archaeal metagenome-assembled genomes (MAGs) were recovered through genome binning from the co-assembly step, including 57 high-quality MAGs (completeness > 95% and contamination <5%) and 189 medium-quality MAGs (completeness > 50% and contamination < 10%). The overall average completeness and contamination were 84% and 2%, respectively. 220 MAGs were classified as bacteria, and the prevalence phyla identified were *Proteobacteria* (46), *Chloroflexi* (37), *Firmicutes* (20), *Planctomycetes* (20),

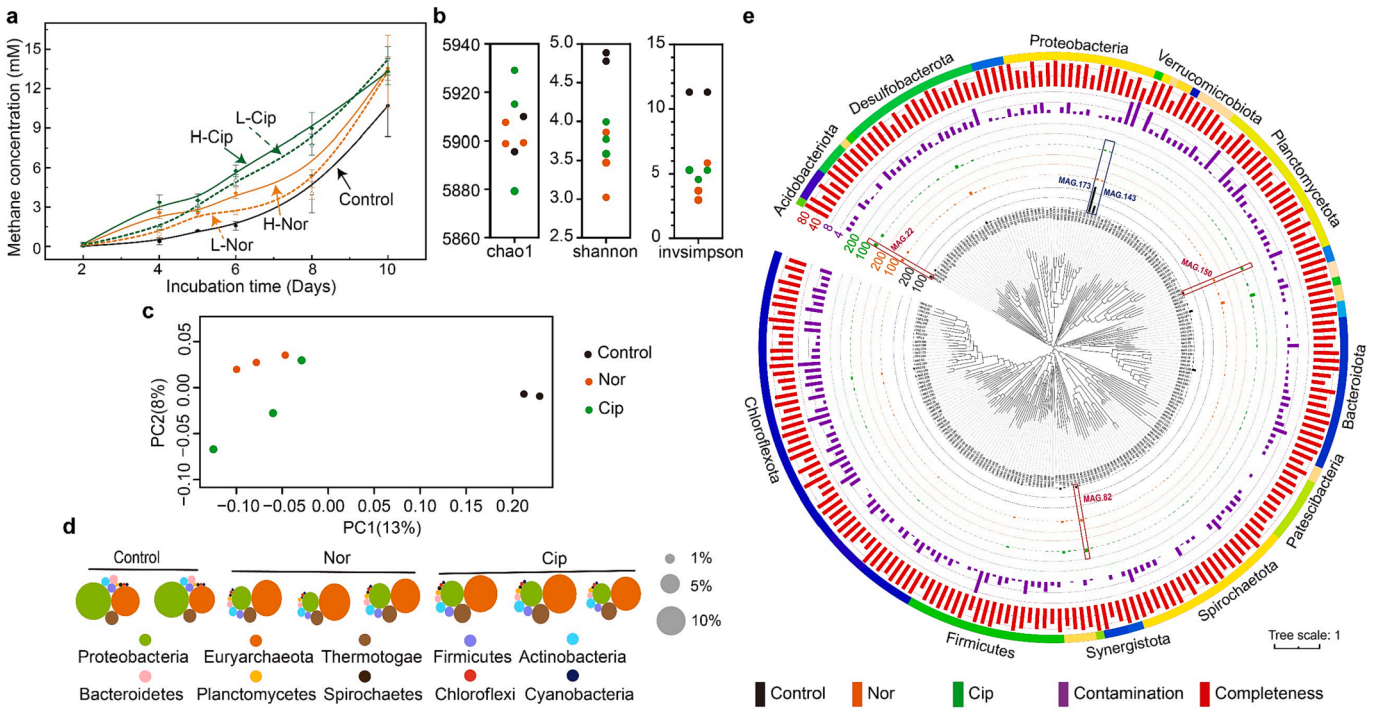

Fig. 1. Antibiotics altered CH_4 production and microbial composition. CH_4 production kinetics under different antibiotics treatments (n=12, a). The α diversity index of each sample obtained from reads classification (n=8, b). The principal coordination analysis of the samples based on their Bray-Curtis distances of reads classification (n=8, c). The proportion of the first ten abundant phyla in each sample (n=8, d). Maximum likelihood phylogenomic tree of the bacterial MAGs (e). The bar layers showed the average abundance (copies per million reads) in each group (black for the control group (n=2), orange for norfloxacin group (n=3), and green for ciprofloxacin group (n=3)); the contamination rate (purple, percentage), and the completeness rate (red, percentage); The color stripe outer ring layer showed the phylum levels with>5 MAGs labeled beside the ring. The blue box showed significantly decreased MAGs, and the red boxes showed significantly increased MAGs. Nor, norfloxacin; L-Nor, low concentration of norfloxacin (50 $mg{\cdot}L^{-1}$); H-Nor, high concentration of norfloxacin (100 $mg{\cdot}L^{-1}$); Cip, ciprofloxacin; L-Cip, low concentration of ciprofloxacin (50 $mg{\cdot}L^{-1}$); H-Cip, high concentration of ciprofloxacin (100 $mg{\cdot}L^{-1}$).

Spirochaetes (20), and *Bacteroidetes* (19) (Figure 1e). The relative abundance of one *Proteobacteria* (MAG.173) sharply decreased with the presence of antibiotics (p = 0.0003 for ciprofloxacin, p = 0.0002 for norfloxacin, Figure 1e). The abundance of other phyla showed slight improvements, such as *Thermotogae* (MAG.82, $p = 0.023$ for ciprofloxacin, $p = 0.042$ for norfloxacin), *Planctomycetes* (MAG.150, $p = 0.037$ for ciprofloxacin, $p = 0.028$ for norfloxacin), and *Nitrospirae* (MAG.22, p = 0.011 for ciprofloxacin, $p = 0.035$ for norfloxacin).

3.3. Co-occurrence networks for bacterial and archaeal genomes

Here, co-occurrence networks were constructed (Figure 2). A total of 245, 243, and 243 nodes were retrieved in the control, norfloxacin, and ciprofloxacin groups, respectively, with similar archaeal and bacterial proportions: 89% for bacteria and 11% for archaea (Figure 2a). The network for the control group contained 3,359 edges (Figure 2b). In contrast, these links sharply decreased to 2,208 and 1021 in the groups with antibiotics (Figure 2b), implying weakened interactions between bacteria and archaea or strong selectivity by methanogens with antibiotic exposure.

Sub-networks among bacterial and the two most abundant methanogen MAGs (MAG.91 and MAG.3) were further retrieved (Figure 2c,d). The sub-networks of *Methanolinea* were constituted with 151 (control), 130 (norfloxacin), and 41 (ciprofloxacin) nodes and 198 (control), 151 (norfloxacin), and 41 (ciprofloxacin) edges. In contrast, the sub-networks of *Methanosaeta* had 221 (control), 60 (norfloxacin), and 48 (ciprofloxacin) nodes and 220 (control), 116 (norfloxacin), and 46 (ciprofloxacin) edges. The number of nodes and edges of both sub-networks decreased in the presence of antibiotics, especially for ciprofloxacin (Figure 2c,d). The proportion of *Methanosaeta*-related links exhibited a similarly decreased trend (7%, 5%, and 5%, Figure 2d), further indicating a simplified co-occurrence relationship between functional bacteria and *Methanosaeta* present in the treatments with antibiotics.

3.4. Genomes for methanation by weak syntrophy via DIET-CO_2 reduction

A phylogenetic analysis based on 120 conserved single-copy genes was performed to identify potential bacteria with DIET capacity (see supplementary material), which may connect a close network with *Methanolinea* and/or *Methanosaeta*. Ten MAGs were placed close to known exoelectrogens, six of which were *Proteobacteria*, with three of them within the *Geobacter* clade. MAG.156 placed in this clade was the most abundant genome and favored by norfloxacin ($p = 0.037$) and ciprofloxacin ($p = 0.021$) (see supplementary material), suggesting a potential DIET-CO_2 reduction progress. However, after further analysis of multiple c-type cytochromes (CytCs) and e-pili, which generally participate in DIET, MAG.156 had only 17 CytCs and 2 MH-CytCs, less than most exoelectrogen candidates (see supplementary material).

Among these 10 MAGs, the critical component of the conductive pilus, PilA, was also shown in their genome, yet its abundance was low and decreased to almost absent with antibiotics. CyCs and MH-CyCs were also identified in MAG.115 of the *Rhodobacter* clade, of which the abundance also decreased with antibiotics ($p = 0.041$ for ciprofloxacin, $p = 0.033$ for norfloxacin). MAG.154 was in third place of CytC numbers and contained two copies of PilA genes, but its abundance was negligible. The overall abundance of CytCs ($p = 0.002$ for ciprofloxacin, $p = 0.003$ for norfloxacin) and PilA ($p = 0.041$ for ciprofloxacin, $p = 0.047$ for norfloxacin) in the microbiomes showed decreasing tendencies with antibiotics treatments.

A phylogenetic analysis was performed with the bacterial MAGs and

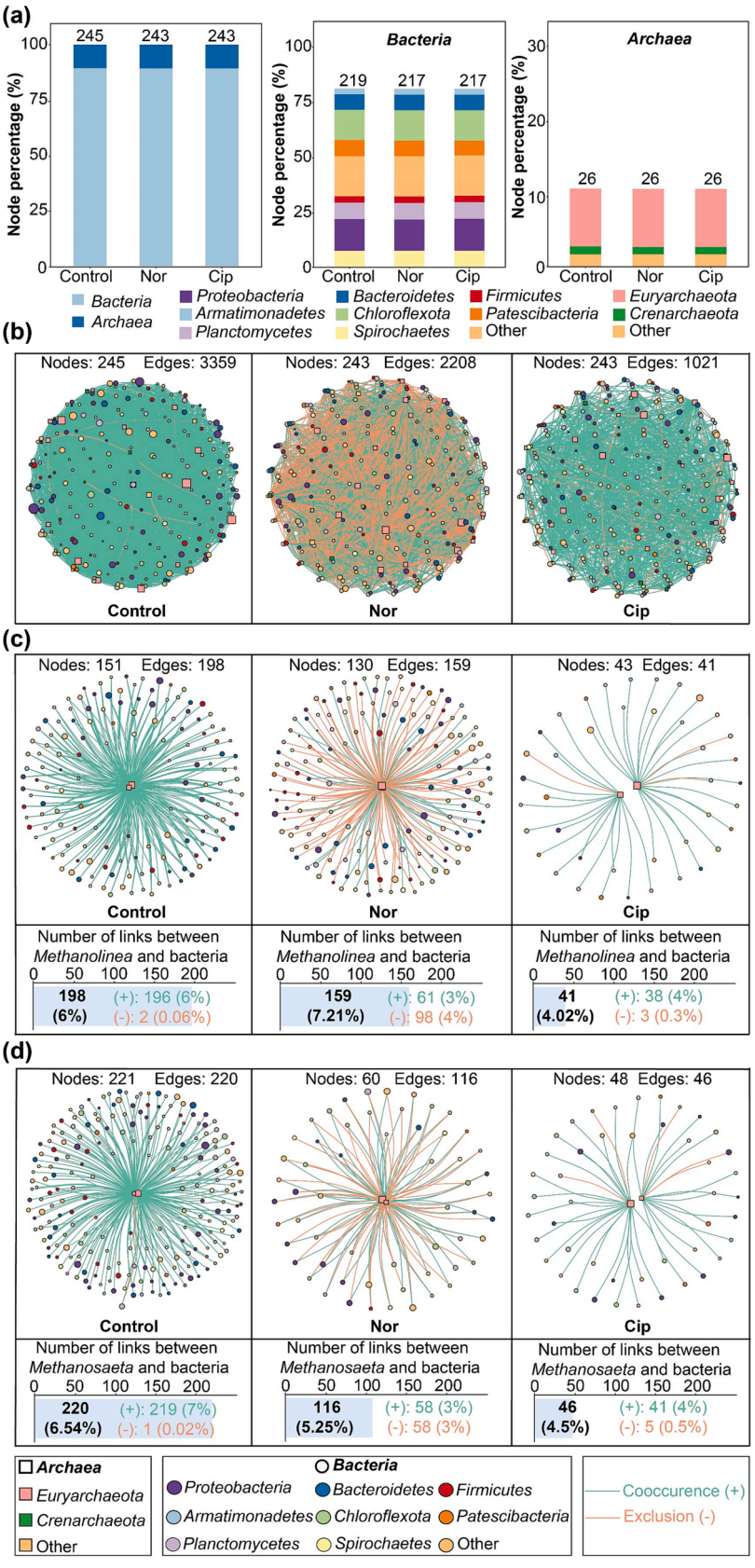

Fig. 2. Co-occurrence networks of MAGs. The percentage of different taxa in the nodes of the networks (a). The total number of nodes was shown on the top of the bars. Networks of bacterial and archaeal MAGs in each group (b). Networks of bacterial and *Methanolinea* MAGs (c). Networks of bacterial and *Methanosaeta* MAGs (d). The percentage in the parentheses showed the proportion of edges linked to *Methanolinea* or *Methanosaeta* in all archaea. Control, control group (n=4); Nor, norfloxacin (n=6); Cip, ciprofloxacin (n=6).

genomes of seven syntrophic acetate-oxidizing bacteria (SAOBs) species from different phyla. Five MAGs were closely placed with known SAOB species, belonging to *Firmicutes*, *Proteobacteria*, and *Thermotogae* (see supplementary material), indicating their acetate oxidizing potential. The most abundant MAG in the control group, MAG.173, was grouped with the experimentally proved SAOB *Thiopseudomonas denitrificans* (see supplementary material). However, the drastic decrease in abundance with the addition of antibiotics ($p = 0.0003$ for ciprofloxacin, $p = 0.0002$ for norfloxacin) suggested that the consumption of acetate diminished (see supplementary material). With very low abundance, some other bins, such as MAG.39 and MAG.103, were grouped with *Clostridium ultunense* (see supplementary material).

CO_2 reduction to generate CH_4 is presently considered a predominant process in artificial digestion systems (Ajay et al., 2020; Noori et al., 2020). Of which, the core pathway is considered to be an increase in DIET. But many studies have only analyzed the 16S rDNA with some signal of potential electricigens (Martins et al., 2018; Van Steendam et al., 2019), and even undetectable of approved electrogenic bacteria (Cui et al., 2021; Qi et al., 2021). No correlation between increased CH_4 generation and electrical conductivity was observed, suggesting that DIET is partly involved at most (Martins et al., 2018). Many investigations lacked direct experimental evidence for the role of DIET in enhancing the anaerobic digestion performance (Van Steendam et al., 2019).

3.5. Genomes for acetate turnover and methanation

Several bacteria regulated by antibiotics were not linked to MIET or DIET through phylogenetic analysis. Their genomic repertoire was explored, and variable metabolic characteristics were found. Most bacteria stimulated by antibiotics were primarily acetate-producing bacteria by degrading macromolecules, such as polysaccharides (MAG.216), lipids (MAG.22), and proteins (MAG.253). Meanwhile, they all contained the first two enzymes of the Wood-Ljungdahl pathway to convert

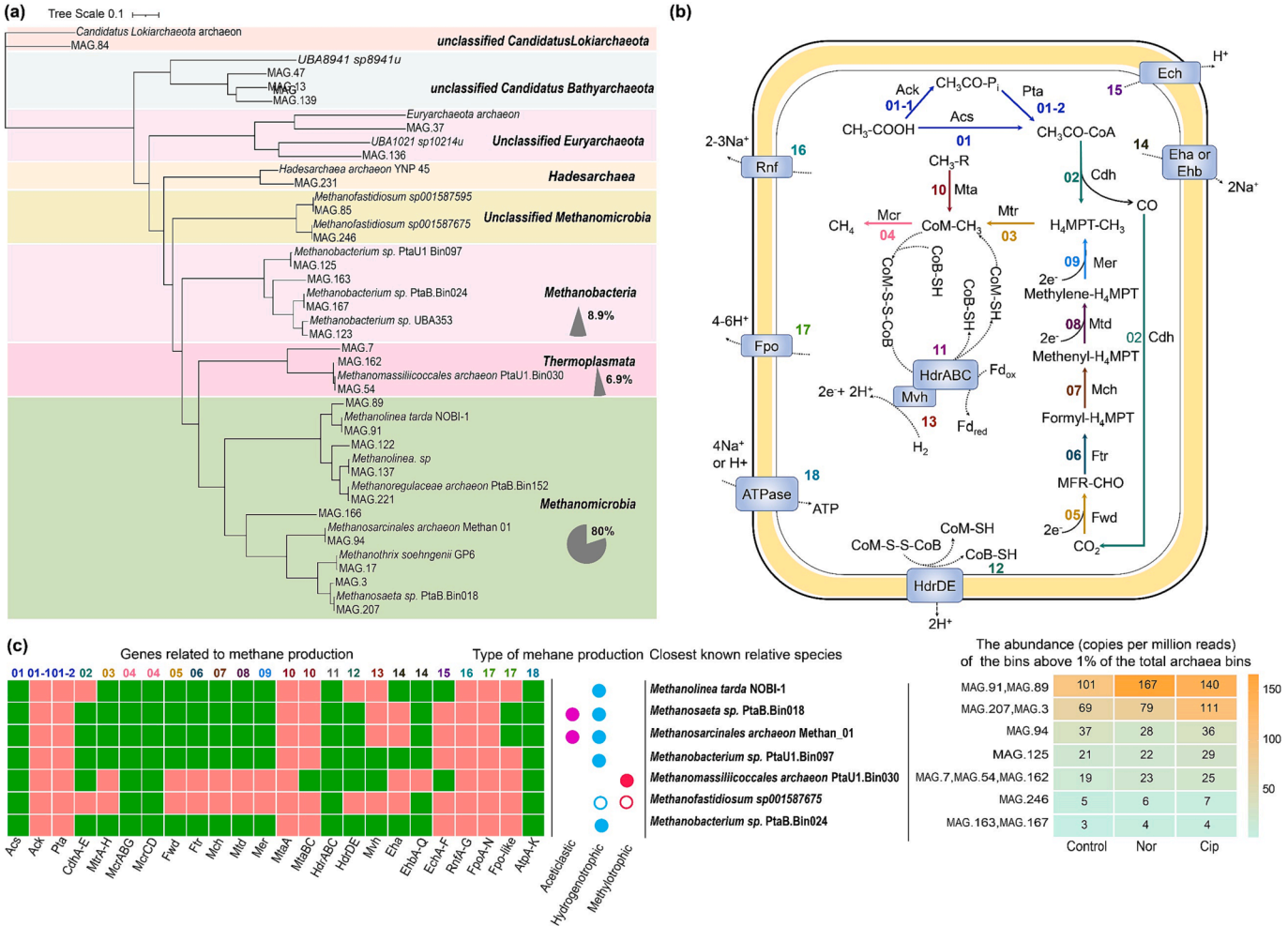

Fig. 3. Potential functional microbes and metabolisms for CH_4 production. Maximum likelihood phylogenomic tree showing closest archaeal relatives of MAGs (a). The grey pie charts showed the proportion of MAGs in the corresponding class. Complete methanogenic pathway and closely related genes (b), marked with different colors and numbers for the reactions. Evaluation of the genes required for methanogenesis and the abundance of methanogens (n=8, c). Only the MAGs above 1% of the total archaea were shown. Green and orange boxes showed the presence and absence of the genes in a genome, respectively. Colored circles: acetoclastic methanogenesis (pink); hydrogenotrophic methanogenesis (light blue); methylotrophic methanogenesis (red). Open circles indicated predicted H_2-dependent methylotrophic methanogenesis. The abundance was the average of two (control group, n=2) or three replicates (antibiotic groups, n=3) and normalized as copies per million reads. Ack, acetate kinase; Acs, acetyl-CoA synthase; CoB-SH, coenzyme B; Cdh, carbon monoxide dehydrogenase-acetyl-CoA synthase complex; CoM-SH, coenzyme M; Ech, energy-conserving hydrogenase; Eha and Ehb, energy-converting hydrogenase A and hydrogenase B; Fd, ferredoxin; Fpo, F_{420}-H_2-dehydrogenase; Ftr, formylmeth-anofuran-H_4MPT formyltransferase; Fwd, formyl-methanofuran dehydrogenase; H_4MPT, tetrahydromethanopterin; Hdr, heterodisulfide reductase; Mch, methenyl-H_4MPT cyclohydrolase; Mcr, methyl-coenzyme M reductase; Mer, F_{420}-dependent methylene-H_4MPT reductase; MFR, methanofuran; Mta, methanol-specific corrinoid protein coenzyme M methyltransferase; Mtd, F_{420}-dependent methylene H_4MPT dehydrogenase; Mtr, Na^+-translocating methyl-H_4MPT-coenzyme-M-methyltransferase; Pta, phosphate acetyltransferase; Rnf, Na^+-translocating ferredoxin-NAD oxidoreductase.

acetate to acetyl-CoA, showing the potential to provide substrates for methanogens. *Methanosaeta* sp PtaB.Bin018 (MAG.207 and MAG.3, Figure 3a), the second most abundant methanogen, contained the required enzymes for acetoclastic pathways (Figure 3b,c). Of particular importance, both antibiotics increased their abundance with the highest stimulated effect from ciprofloxacin (p = 0.003 for ciprofloxacin, p = 0.023 for norfloxacin, Figure 3c).

3.6. Prevalent acetoclastic methanogenesis evidenced through isotopic analysis

To link CH_4 production to its precursor, ^{13}C values of CH_4 and CO_2 were analyzed on the 6th, 8th, and 10th day (Figure 4a). There was no difference in $\delta^{13}C$-CH_4 between the antibiotic-containing and original artificial wastewater with values around -40‰ (Figure 4a), the typical CH_4 sources for acetoclastic methanogenesis. The α values were all below 1.030 at the mid-term of the experiment and maintained at around 1.02 at the late stage (Figure 4b). The natural abundance of carbon isotope fraction experiment showed typical $\delta^{13}C$-CH_4 and α values ranging in acetoclastic methanogenesis (Conrad et al., 2021; Conrad and Klose, 2011; Xiao et al., 2020b), implying that ciprofloxacin acted as a positive motivating factor on acetate disproportionation followed by norfloxacin.

When applying the acetoclastic methanogenesis inhibitor methyl fluoride (CH_3F), the acetate consumption (see supplementary material) and CH_4 production (see supplementary material) were severely reduced. CH_3F, an inhibitor of acetoclastic methanogenesis, significantly reduced the efficiency of CH_4 production by an order of magnitude. Furthermore, the isotope tracing analysis showed that ^{13}C-CH_4 abundance was positively correlated with CH_4 concentration (see supplementary material), confirming that the methyl group of acetate was markedly transferred to CH_4 rather than CO_2 (Li et al., 2018; Xiao et al., 2020b). Thus, acetate was directly cleaved to CH_4 and CO_2, rather than oxidized to two CO_2 in this study. Increasing evidence already suggests that acetate-dependent methanogenesis is significantly enhanced by some conductive materials during anaerobic digestion, whereas CO_2-dependent methanogenesis is reduced (Lü et al., 2020; Yu et al., 2022).

To validate these results from natural carbon, isotope-marked substrates (3% and 6% $^{13}CH_3COONa$) were used. The CH_4 production scenarios were similar between 3% and 6% $^{13}CH_3COONa$ (Figure 5a,b), indicating the reliable performance of the floxacin in promoting methanogenesis. In general, CH_4 produced in the original wastewater without antibiotics had a low ^{13}C abundance (Figure 5c,d). For example, for the 3% $^{13}CH_3COONa$ treatment, ^{13}C-CH_4 abundance in the middle (day 15) and end (day 21) was about 2% and 3%, respectively (Figure 5c). When the abundance of $^{13}CH_3COONa$ doubled, ^{13}C-CH_4 was about 3% and 8%, respectively (Figure 5d). Antibiotics significantly increased $^{13}CH_4$ abundance, with ciprofloxacin showing the highest performance reaching 12% (Figure 5c,d). For both $^{13}CH_3COONa$ addition treatments, CH_4 yield and ^{13}C-CH_4 abundance showed a close positive correlation (p = 0.0001 and 0.0003, respectively; see supplementary material). Remarkably, ^{13}C-CH_4 isotope strongly predicted CH_4 production rates (R^2 = 0.779 and 0.828, respectively; see supplementary material).

Compared with ^{13}C-CH_4 abundance, the ^{13}C-CO_2 abundance was very low. No difference in ^{13}C-CO_2 abundance was detected between antibiotic-containing and original wastewater (Figure 5e,f). In the 3% of $^{13}CH_3COONa$ treatment, ^{13}C-CO_2 was below 1%, typical natural abundance, as well as in the presence of highly ^{13}C-labelled sodium acetate (Figure 5e). Similarly, it also maintained a relatively stable and low value under 6% in the $^{13}CH_3COONa$ treatment (Figure 5f). Based on Pearson analysis of CH_4 concentration and ^{13}C-CO_2 abundance, no correlation between increased CH_4 yield and CO_2 reduction for methanation was observed (p = 0.864 and 0.705, respectively; see supplementary material).

If the CH_4 production process is completed via the acetoclastic methanogenesis alone in an acetate-rich environment, the energy obtained can be fully utilized by methanogens. However, if it comes from DIET-CO_2 reduction, the same small amount of energy needs to be shared by two kinds of cooperative microorganisms, fermentative bacteria and methanogenic archaea (Roy et al., 2022; Xiao et al., 2020b). Combined with the energy release of methanogenic archaea, acetoclastic methanogenesis releases more energy than CO_2 reduction in a nominal environment. According to the data from a previous study (Bethke et al., 2011), when 1 mol of CH_4 is produced, 32 or 1 kJ of

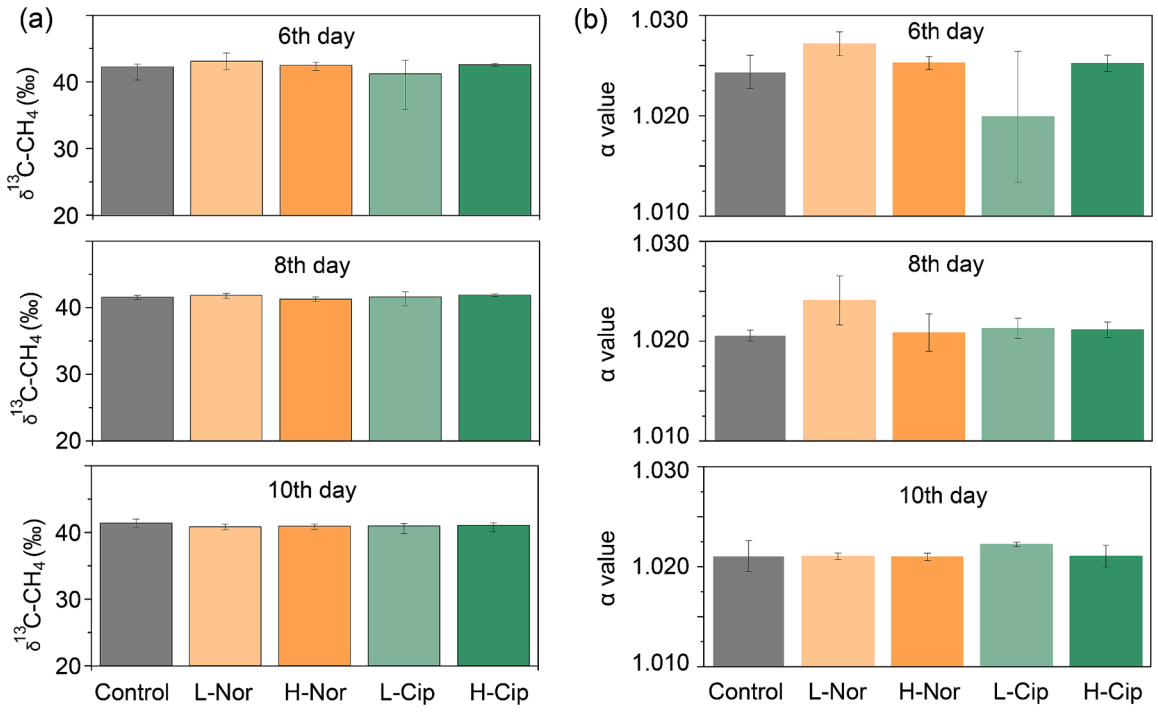

Fig. 4. Isotopic of CH_4. $\delta^{13}C$-CH_4 (a) and α value (b) in natural carbon isotope fraction. Control, control group (n=3); L-Nor: low concentration of norfloxacin (n=3); H-Nor: high concentration of norfloxacin (n=3); L-Cip: low concentration of ciprofloxacin (n=3); H-Cip: high concentration of ciprofloxacin (n=3).

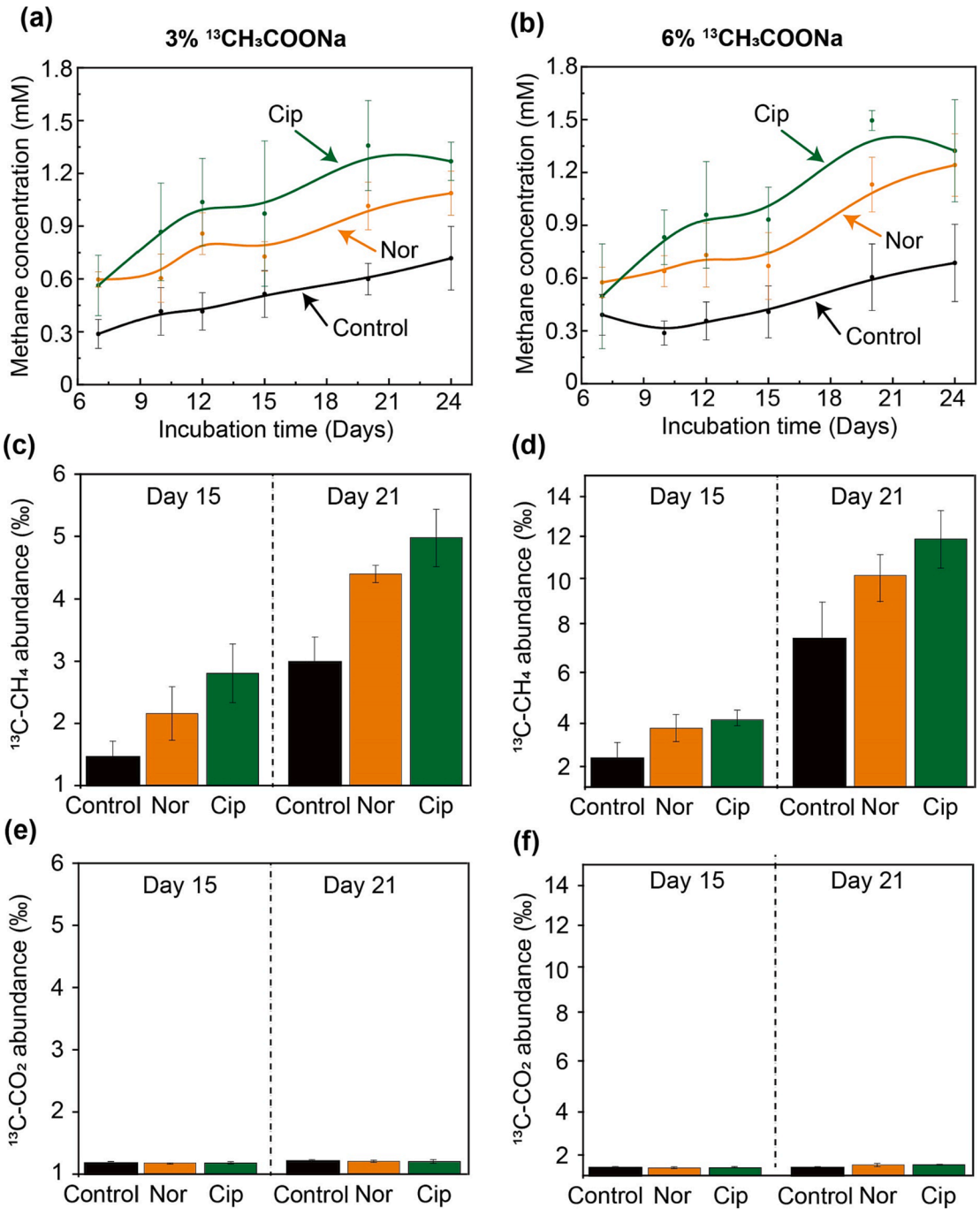

Fig. 5. CH_4 production scenario at room temperature with 3% and 6% $^{13}CH_3COONa$ as isotope marked substrates. CH_4 production kinetics (a, b), ^{13}C-CH_4 (c, d), and ^{13}C-CO_2 (e, f) abundance with the presence of 3% and 6% $^{13}CH_3COONa$, respectively. Wastewater with 3% $^{13}CH_3COONa$ (a, c, e), wastewater with 6% $^{13}CH_3COONa$ (b, d, f). Data in c, d, e, and f were collected on day 15 (left half) and 21 (right half). Control, control group (n=3); Nor, norfloxacin (n=3); Cip, ciprofloxacin (n=3).

energy is available by acetoclastic methanogenesis or hydrogenotrophic methanogenesis, respectively. In the present study, CO_2 reduction seems to be not the optimal option in terms of survival strategy.

The findings in this work underscore the contribution of acetoclastic methanogenesis to CH_4 production during anaerobic digestion through genome-centric and isotope tracing, implicating that more direct evidence should be taken into account during the research of biomethane production. Nevertheless, this work has certain limits. The experiment was carried out with mimic wastewater at the microcosm level. Studies with industrial bioreactors and real wastewater should be taken in the future.

4. Conclusion

Methanosaeta acted as the leading CH_4 producer. The category of acetate-consuming bacteria showed decreased numbers in wastewaters with antibiotics as well as their proportions in the sub-networks. Herein, the ratio of acetogenic MAGs was enhanced several folds by antibiotics. Methanogens tended to complete methanogenesis and were inspired by acetogenic bacteria. Therefore, it is pertinent that future laboratory or in-situ experimentation should attach importance to acetate turnover to better optimize wastewater treatment and energy recovery strategy.

CRediT authorship contribution statement

Jian Liu: Data curation, Visualization, Writing – original draft. **Jiafeng Yu:** Methodology, Funding acquisition, Data curation. **Yang Tan:** Data curation, Methodology. **Run Dang:** Data curation, Formal analysis. **Meng Zhou:** Methodology, Data curation. **Marcela Hernández:** Validation, Writing – review & editing. **Eric Lichtfouse:** Data curation, Validation, Writing – review & editing. **Leilei Xiao:** Resources, Funding acquisition, Conceptualization, Methodology.

Declaration of Competing Interest

The authors declare that they have no known competing financial interests or personal relationships that could have appeared to influence the work reported in this paper.

Data availability

All the links have been shared in the Data availability statement (below)

Acknowledgements

This work was supported by Youth Innovation Promotion Association, CAS (2021213), the National Natural Science Foundation of China (42077025, 42277236), the Youth Science and Technology Innovation Plan of Universities in Shandong (2019KJE007).

Data availability statement

All data needed to evaluate the conclusions in the paper are present in the paper and/or the Supplementary Materials. The metagenomic sequencing data have been deposited in the National Center for Biotechnology Information (NCBI) Short Read Archive database (SRA, https://www.ncbi.nlm.nih.gov/bioproject/PRJNA734822).

Appendix A. Supplementary data

Supplementary data to this article can be found online at https://doi.org/10.1016/j.biortech.2023.129589.

References

Ajay, C.M., Mohan, S., Dinesha, P., Rosen, M.A., 2020. Review of impact of nanoparticle additives on anaerobic digestion and methane generation. Fuel 277, 118234.
Bethke, C.M., Sanford, R.A., Kirk, M.F., Jin, Q., Flynn, T.M., 2011. The thermodynamic ladder in geomicrobiology. Am. J. Sci. 311 (3), 183–210.
Cavalcante, W.A., Gehring, T.A., Zaiat, M., 2021. Stimulation and inhibition of direct interspecies electron transfer mechanisms within methanogenic reactors by adding magnetite and granular actived carbon. Chem. Eng. J. 415, 128882.
Chen, L.-X., Anantharaman, K., Shaiber, A., Eren, A.M., Banfield, J.F., 2020. Accurate and complete genomes from metagenomes. Genome Res. 30 (3), 315–333.
Conrad, R., 2005. Quantification of methanogenic pathways using stable carbon isotopic signatures: A review and a proposal. Org Geochem. 36 (5), 739–752.
Conrad, R., Klose, M., 2011. Stable carbon isotope discrimination in rice field soil during acetate turnover by syntrophic acetate oxidation or acetoclastic methanogenesis. Geochim. Cosmochim. Acta 75 (6), 1531–1539.
Conrad, R., Liu, P., Claus, P., 2021. Fractionation of stable carbon isotopes during acetate consumption by methanogenic and sulfidogenic microbial communities in rice paddy soils and lake sediments. Biogeosciences 18, 6533–6546.
Cui, Y., Mao, F., Zhang, J., He, Y., Tong, Y.W., Peng, Y., 2021. Biochar enhanced high-solid mesophilic anaerobic digestion of food waste: Cell viability and methanogenic pathways. Chemosphere 272, 129863.
De Bernardini, N., Basile, A., Zampieri, G., Kovalovszki, A., De Diego Diaz, B., Offer, E., Wongfaed, N., Angelidaki, I., Kougias, P.G., Campanaro, S., Treu, L., 2022. Integrating metagenomic binning with flux balance analysis to unravel syntrophies in anaerobic CO_2 methanation. Microbiome. 10, 117.
Dong, D., Kyung Choi, O.h., Woo Lee, J., 2022. Influence of the continuous addition of zero valent iron (ZVI) and nano-scaled zero valent iron (nZVI) on the anaerobic biomethanation of carbon dioxide. Chem. Eng. J. 430, 132233.
Etminan, M., Myhre, G., Highwood, E.J., Shine, K.P., 2016. Radiative forcing of carbon dioxide, methane, and nitrous oxide: A significant revision of the methane radiative forcing. Geophys. Res. Lett. 43, 12614–12623.
Guo, Q., Wang, Y., Qian, J., Zhang, B., Hua, M., Liu, C., Pan, B., 2021. Enhanced production of methane in anaerobic water treatment as mediated by the immobilized fungi. Water Res. 190, 116761.
Holmes, D.E., Smith, J.A., 2016. Biologically produced methane as a renewable energy source. Adv. Appl. Microbiol. 97, 1–61.
Hua, H., Jiang, S., Yuan, Z., Liu, X., Zhang, Y., Cai, Z., 2022. Advancing greenhouse gas emission factors for municipal wastewater treatment plants in China. Environ. Pollut. 295, 118648.
Hultman, J., Waldrop, M.P., Mackelprang, R., David, M.M., McFarland, J., Blazewicz, S. J., Harden, J., Turetsky, M.R., McGuire, A.D., Shah, M.B., VerBerkmoes, N.C., Lee, L. H., Mavrommatis, K., Jansson, J.K., 20Multi-omics of permafrost, active layer and thermokarst bog soil microbiomes. Nature. 2015 521:7551 521, 208–212.
IEA, Global Energy Review 2021, https://www.iea.org/reports/global-energy-review-2021 (accessed 7.9.23).
Ipcc, 2014. Climate change 2014: Synthesis report. Cambridge University Press, Cambridge.
Jin, H.-Y., He, Z.-W., Ren, Y.-X., Tang, C.-C., Zhou, A.-J., Liu, W., Liang, B., Li, Z.-H., Wang, A., 2022. Current advances and challenges for direct interspecies electron transfer in anaerobic digestion of waste activated sludge. Chem. Eng. J. 450, 137973.
Kumar, V., Nabaterega, R., Khoei, S., Eskicioglu, C., 2021. Insight into interactions between syntrophic bacteria and archaea in anaerobic digestion amended with conductive materials. Renew. Sustain. Energy Rev. 144, 110965.
Langbehn, R.K., Michels, C., Soares, H.M., 2021. Antibiotics in wastewater: From its occurrence to the biological removal by environmentally conscious technologies. Environ. Pollut. 275, 116603.
Li, J., Xiao, L., Zheng, S., Zhang, Y., Luo, M., Tong, C., Xu, H., Tan, Y., Liu, J., Wang, O., Liu, F., 2018. A new insight into the strategy for methane production affected by conductive carbon cloth in wetland soil: Beneficial to acetoclastic methanogenesis instead of CO_2 reduction. Sci. Total Environ. 643, 1024–1030.
Lü, C., Shen, Y., Li, C., Zhu, N., Yuan, H., 2020. Redox-active biochar and conductive graphite stimulate methanogenic metabolism in anaerobic digestion of waste-activated sludge: Beyond direct interspecies electron transfer. ACS Sustain. Chem. Eng. 8 (33), 12626–12636.
Mancini, E., Tian, H., Angelidaki, I., Fotidis, I.A., 2021. The implications of using organic-rich industrial wastewater as biomethanation feedstocks. Renew. Sustain. Energy Rev. 144, 110987.
Martins, G., Salvador, A.F., Pereira, L., Alves, M.M., 2018. Methane production and conductive materials: A critical review. Environ. Sci. Tech. 52 (18), 10241–10253.
Mitchell, S.M., Ullman, J.L., Teel, A.L., Watts, R.J., Frear, C., 2013. The effects of the antibiotics ampicillin, florfenicol, sulfamethazine, and tylosin on biogas production and their degradation efficiency during anaerobic digestion. Bioresour. Technol. 149, 244–252.
Noori, M.T., Vu, M.T., Ali, R.B., Min, B., 2020. Recent advances in cathode materials and configurations for upgrading methane in bioelectrochemical systems integrated with anaerobic digestion. Chem. Eng. J. 392, 123689.
Prakash, D., Chauhan, S.S., Ferry, J.G., 2019. Life on the thermodynamic edge: Respiratory growth of an acetotrophic methanogen. Sci. Adv. 5, eaaw9059.
Qi, Q., Sun, C., Zhang, J., He, Y., Wah Tong, Y., 2021. Internal enhancement mechanism of biochar with graphene structure in anaerobic digestion: The bioavailability of trace elements and potential direct interspecies electron transfer. Chem. Eng. J. 406, 126833.
Rotaru, A.-E., Shrestha, P.M., Liu, F., Shrestha, M., Shrestha, D., Embree, M., Zengler, K., Wardman, C., Nevin, K.P., Lovley, D.R., 2014. A new model for electron flow during anaerobic digestion: direct interspecies electron transfer to *Methanosaeta* for the reduction of carbon dioxide to methane. Energ. Environ. Sci. 7 (1), 408–415.
Roy, C.K., Toya, S., Hoshiko, Y., Sabidi, S., Mustapha, N.A., Miyazaki, T., Maeda, T., 2022. Effect of sodium tungstate on anaerobic digestion of waste sewage sludge: Enhanced methane production via increased acetoclastic methanogens. J. Environ. Chem. Eng. 10 (3), 107524.
Saunois, M., Stavert, A.R., Poulter, B., Bousquet, P., Canadell, J.G., Jackson, R.B., Raymond, P.A., Dlugokencky, E.J., Houweling, S., Patra, P.K., Ciais, P., Arora, V.K., Bastviken, D., Bergamaschi, P., Blake, D.R., Brailsford, G., Bruhwiler, L., Carlson, K. M., Carrol, M., Castaldi, S., Chandra, N., Crevoisier, C., Crill, P.M., Covey, K., Curry, C.L., Etiope, G., Frankenberg, C., Gedney, N., Hegglin, M.I., Höglund-Isaksson, L., Hugelius, G., Ishizawa, M., Ito, A., Janssens-Maenhout, G., Jensen, K.M., Joos, F., Kleinen, T., Krummel, P.B., Langenfelds, R.L., Laruelle, G.G., Liu, L., Machida, T., Maksyutov, S., McDonald, K.C., McNorton, J., Miller, P.A., Melton, J.R., Morino, I., Müller, J., Murguia-Flores, F., Naik, V., Niwa, Y., Noce, S., O'Doherty, S., Parker, R.J., Peng, C., Peng, S., Peters, G.P., Prigent, C., Prinn, R., Ramonet, M., Regnier, P., Riley, W.J., Rosentreter, J.A., Segers, A., Simpson, I.J., Shi, H., Smith, S. J., Steele, L.P., Thornton, B.F., Tian, H., Tohjima, Y., Tubiello, F.N., Tsuruta, A., Viovy, N., Voulgarakis, A., Weber, T.S., van Weele, M., van der Werf, G.R., Weiss, R. F., Worthy, D., Wunch, D., Yin, Y.i., Yoshida, Y., Zhang, W., Zhang, Z., Zhao, Y., Zheng, B.o., Zhu, Q., Zhu, Q., Zhuang, Q., 2020. The global methane budget 2000–2017. Earth Syst. Sci. Data 12 (3), 1561–1623.
Song, X., Liu, J., Jiang, Q., Zhang, P., Shao, Y., He, W., Feng, Y., 2019. Enhanced electron transfer and methane production from low-strength wastewater using a new granular activated carbon modified with nano-Fe_3O_4. Chem. Eng. J. 374, 1344–1352.
Stams, A.J.M., Plugge, C.M., 2009. Electron transfer in syntrophic communities of anaerobic bacteria and archaea. Nat. Rev. Microbiol. 7 (8), 568–577.
Tang, T., Liu, M., Du, Y.e., Chen, Y., 2022. Deciphering the internal mechanisms of ciprofloxacin affected anaerobic digestion, its degradation and detoxification mechanism. Sci. Total Environ. 842, 156718.

Van Steendam, C., Smets, I., Skerlos, S., Raskin, L., 2019. Improving anaerobic digestion via direct interspecies electron transfer requires development of suitable characterization methods. Curr. Opin. Biotechnol. 57, 183–190.
Wang, W., Lee, D.-J., 2021. Direct interspecies electron transfer mechanism in enhanced methanogenesis: A mini-review. Bioresour. Technol. 330, 124980.
Wang, M., Ren, P., Wang, Y., Cai, C., Liu, H., Dai, X., 2022. Erythromycin stimulates rather than inhibits methane production in anaerobic digestion of antibiotic fermentation dregs. Sci. Total Environ. 807, 151007.
Xiao, L., Liu, F., Lichtfouse, E., Zhang, P., Feng, D., Li, F., 2020. Methane production by acetate dismutation stimulated by *Shewanella oneidensis* and carbon materials: An alternative to classical CO2reduction. Chem. Eng. J. 389, 124469.
Xiao, L., Zheng, S., Lichtfouse, E., Luo, M., Tan, Y., Liu, F., 2020. Carbon nanotubes accelerate acetoclastic methanogenesis: From pure cultures to anaerobic soils. Soil Biol. Biochem. 150, 107938.
Xiao, L., Lichtfouse, E., Kumar, P.S., Wang, Q., Liu, F., 2021. Biochar promotes methane production during anaerobic digestion of organic waste. Environ. Chem. Lett. 19 (5), 3557–3564.
Xiao, L., Wang, Y., Lichtfouse, E., Li, Z., Kumar, P.S., Liu, J., Feng, D., Yang, Q., Liu, F., 2021. Effect of antibiotics on the microbial efficiency of anaerobic digestion of wastewater: A review. Front. Microbiol. 11, 611613.
Yang, S., Chen, Z., Wen, Q., 2021. Impacts of biochar on anaerobic digestion of swine manure: Methanogenesis and antibiotic resistance genes dissemination. Bioresour. Technol. 324, 124679.
Yu, J., Liu, J., Senthil Kumar, P., Wei, Y., Zhou, M., Vo, D.-V., Xiao, L., 2022. Promotion of methane production by magnetite via increasing acetogenesis revealed by metagenome-assembled genomes. Bioresour. Technol. 345, 126521.
Zeng, S., Sun, J., Chen, Z., Xu, Q., Wei, W., Wang, D., Ni, B.-J., 2021. The impact and fate of clarithromycin in anaerobic digestion of waste activated sludge for biogas production. Environ. Res. 195, 110792.
Zhang, M., Liu, Y.-S., Zhao, J.-L., Liu, W.-R., Chen, J., Zhang, Q.-Q., He, L.-Y., Ying, G.-G., 2021. Variations of antibiotic resistome in swine wastewater during full-scale anaerobic digestion treatment. Environ. Int. 155, 106694.
Zhi, S., Li, Q., Yang, F., Yang, Z., Zhang, K., 2019. How methane yield, crucial parameters and microbial communities respond to the stimulating effect of antibiotics during high solid anaerobic digestion. Bioresour. Technol. 283, 286–296.
Zhi, S., Zhang, K., 2019. Antibio+-tic residues may stimulate or suppress methane yield and microbial activity during high-solid anaerobic digestion. Chem. Eng. J. 359, 1303–1315.

Supplementary materials for

Acetate cleavage not direct interspecies electron transfer controls methane production revealed by carbon isotope tracing and genome-centric view

Jian Liu[1#], Jiafeng Yu[1#], Yang Tan[2], Run Dang[2], Meng Zhou[3], Marcela Hernández[4], Eric Lichtfouse[5], Leilei Xiao[2]*

[1] Shandong Key Laboratory of Biophysics, Institute of Biophysics, Dezhou University, Dezhou, 253023, P.R. China.

[2] CAS Key Laboratory of Coastal Environmental Processes and Ecological Remediation, Yantai Institute of Coastal Zone Research, Chinese Academy of Sciences, Yantai 264003, P.R. China.

[3] State Key Laboratory of Black Soils Conservation and Utilization, Northeast Institute of Geography and Agroecology, Chinese Academy of Sciences, Harbin 150081, P.R. China

[4] School of Biological Sciences, University of East Anglia, Norwich NR4 7TJ, UK.

[5] State Key Laboratory of Multiphase Flow in Power Engineering, International Research Center for Renewable Energy, Xi'an Jiaotong University, Xi'an, Shaanxi, 710049, P.R. China

* To whom correspondence should be sent:

Leilei Xiao, Yantai Institute of Coastal Zone Research, 17 Chunhui Road, Laishan District, Yantai, Shandong 264003, China. Office number: +86 05352109269, Email: llxiao@yic.ac.cn.

This file includes:

Supplementary Methods, Figure S1-S4, Table S1-S4

Figures

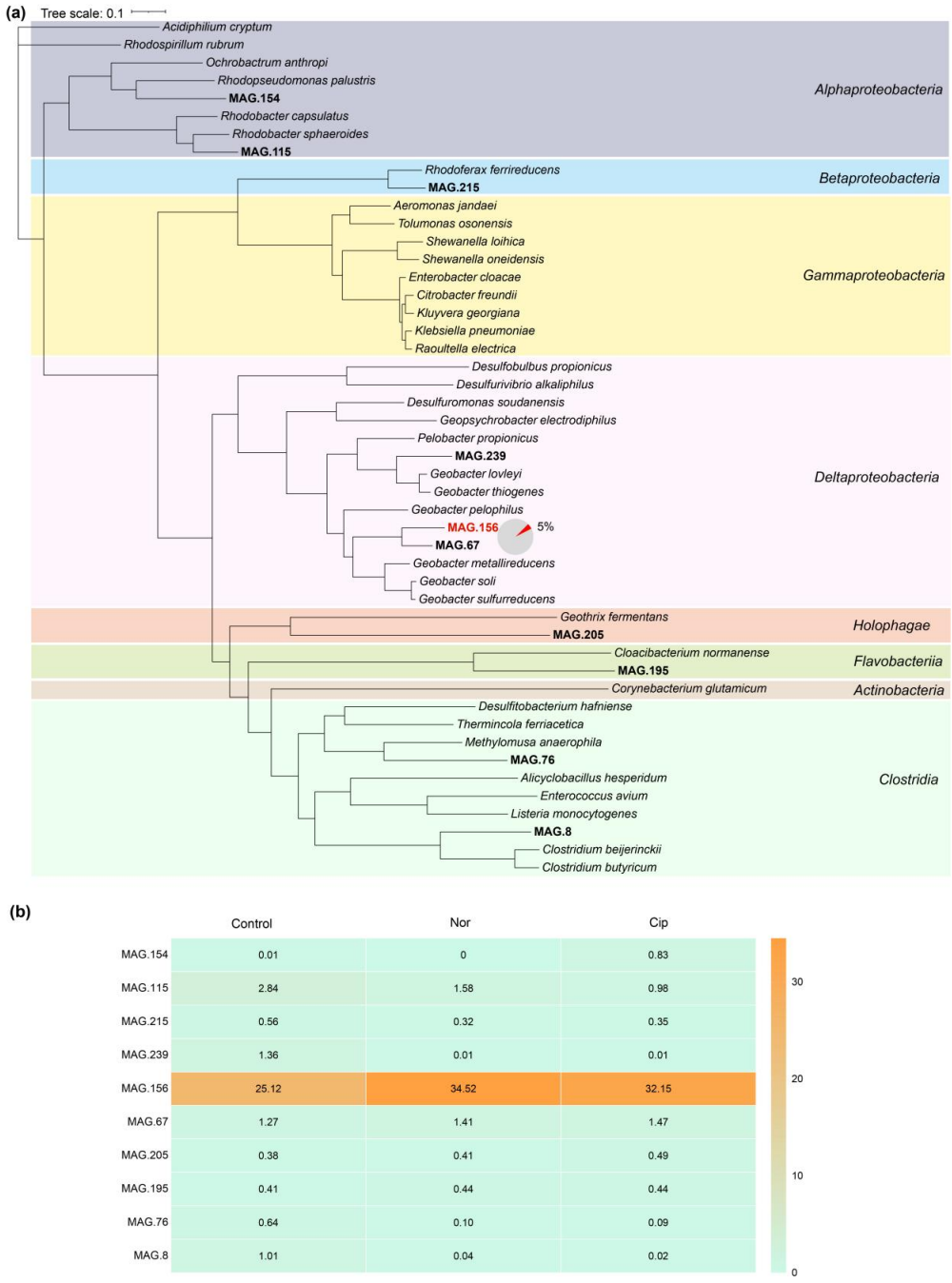

Figure S1 Evaluation of potential electricigens. Maximum likelihood phylogenomic tree showing MAGs close to known electricigens (a). The pie chart showed proportion of bacteria bins. The bin in red was with the most abundant. The abundance of the potential electricity producing MAGs (b). The numbers showed the average of three replicates in each group normalized as copies per million reads.

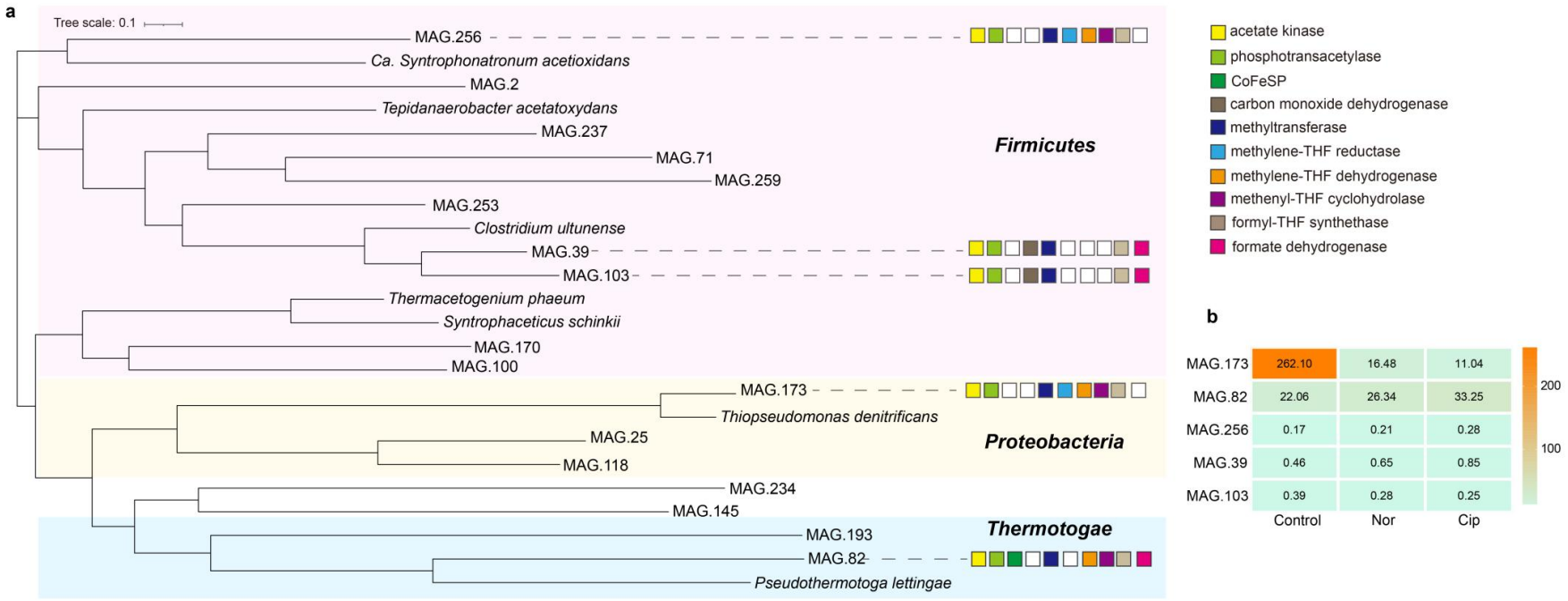

Figure S2 Evaluation of potential syntrophic acetate-oxidizing bacteria (SAOB). A Maximum likelihood phylogenomic tree showing MAGs closed to known SAOB (a). The coloured square showing presence (colour) or absence (white) of the WL pathway genes in the corresponding MAGs. The abundance of the potential SAOB (b). The numbers showed the average of three replicates in each group, which were normalized as copies per million reads.

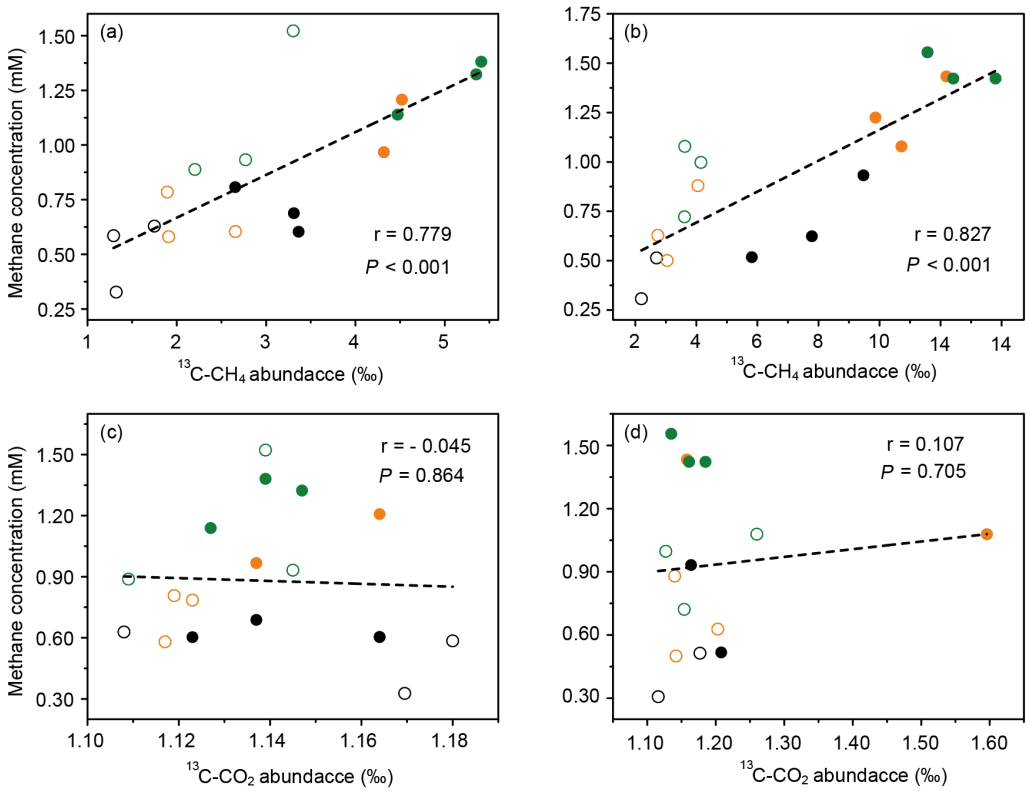

Figure S3 Correlation between CH_4 concentration and ^{13}C abundance. ^{13}C-CH_4 (a, b) showed positive correlation with CH_4 production with 3% (a) and 6% (b) ^{13}C-CH_3COONa. ^{13}C-CO_2 abundance (c, d) had no relationship with CH_4 production.

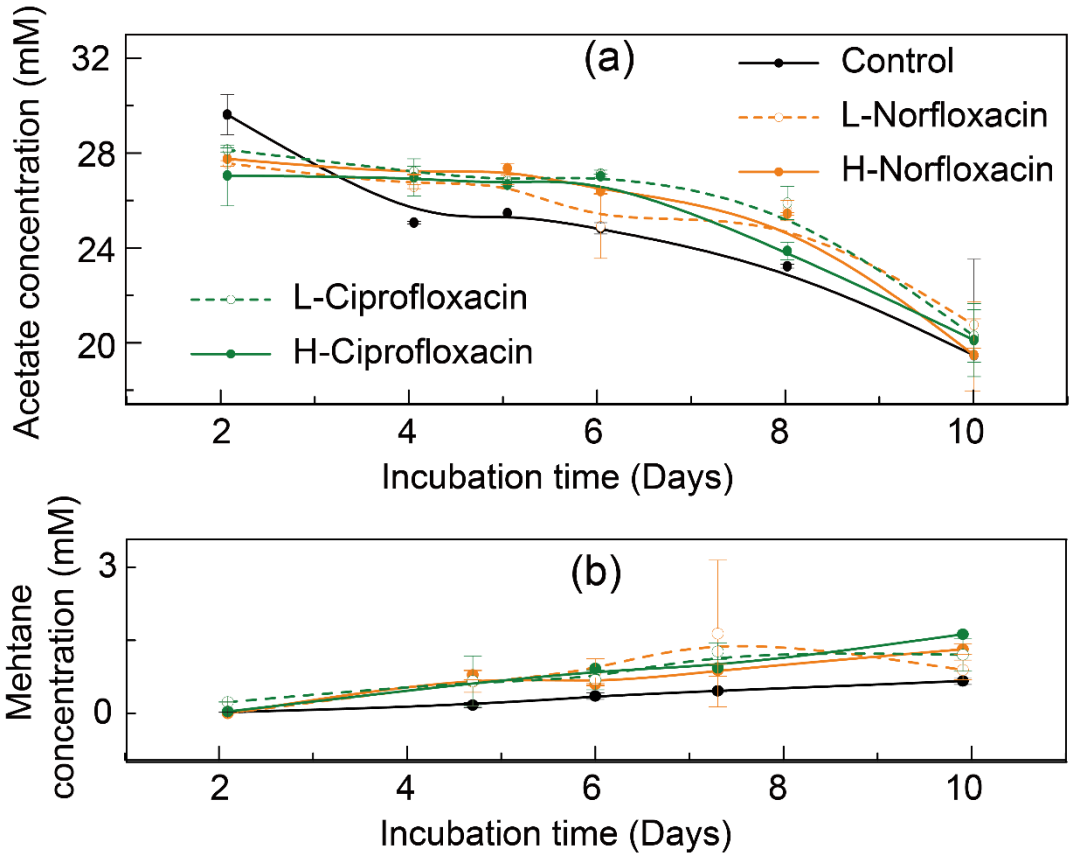

Figure S4 Acetate (a) and methane (b) kinetics under different concentration of antibiotics with acetoclastic methanogenesis inhibitor CH_3F.

Tables

Table S1 Number of different MAGs linked with *Methanosaeta*.

MAGs	Control	Nor	Cip
Acetogenic bacteria	58	18	11
Anaerolineales	21	6	2
Syntrophobacterales	16	6	4
Phycisphaerae	16	4	3
Spirochaetales	5	2	2
Exoelectrogens	9	1	1
Geobacterales	3	1	1
Rhodobacterales	1	0	1
Burkholderiales	1	0	0
Bacteroidetes	1	0	0
Acidobacteriota	1	0	0
Firmicutes	2	0	0
SAOBs	5	1	0
Clostridiales	3	0	0
Pseudomonadales	1	0	0
Thermotogales	1	1	0
Percentage of Acetogenic MAGs (%)	26.2	30	22.9
Percentage of Acetate consumption MAGs (%)	6.3	3.3	2.1
Ratio of Acetogenic/Acetate consumption MAGs	4.14	9	11